Turkish Journal of Engineering & Environmental Sciences

http://journals.tubitak.gov.tr/engineering/

Research Article

Turkish J Eng Env Sci
(2014) 38: 382 – 391

doi:10.3906/muh-1206-5

# Effect of normal stress and relative compaction on secant friction angle of sands

**Seyed Mohammad Reza HOSSEINI***, **Mehrab JESMANI**
Department of Civil Engineering, Imam Khomeini International University, Qazvin, Iran

**Received:** 14.06.2012 • **Accepted/Published Online:** 01.10.2015 • **Printed:** 04.03.2016

**Abstract:** In most geotechnical projects the linear Mohr–Coulomb envelope is used. This envelope is curved for coarse-grained soils and is affected by some factors such as confining pressure, relative density, mineralogy, particle crushing, fine content, and gradation of sand particles. The curved strength envelope could be used to study the behavior of deep foundations, earth dams, soil slopes, and other earth structures in which failure occurs under considerable normal stresses. A deep failure surface may be more critical than a shallow surface when the phenomenon of curved strength envelopes is considered, because the secant friction angle decreases with increasing depth of soil layers and confining pressure. The main purpose of this research is to express the secant friction angle of sands as a function of normal stress and relative compaction. In this study, direct shear tests are performed on air-dried and saturated sand samples at different normal stresses to evaluate the variation of secant friction angle with these factors.

**Key words:** Dilatancy, secant friction angle, normal stress level, relative compaction

## 1. Introduction

In most geotechnical problems, assessment of shear strength of soil or rock is necessary, e.g., bearing capacity or slope stability analysis. The most common representation of shear strength of soils is done by using the linear Mohr–Coulomb envelope that has two components: friction angle and cohesion. In many practical projects it is assumed that these two components are constant and independent of stress level. Some researchers have investigated the factors that affect the friction angle. The author of [1] performed triaxial tests on standard Ottawa sand in order to evaluate the effect of normal stress on friction angle and found that for the loose state (initial void ratio approximately 0.66) the value of secant $\varphi$ decreased from 30° to less than 27° when the confining pressure was increased from 48 kPa to 766 kPa. Similarly, for the dense state, secant $\varphi$ decreased from approximately 34.5° to about 29° due to the same increase in confining pressure. It was established in the literature that friction angle of coarse-grained soils is composed of two components, basic friction angle and dilatancy, where dilatancy angle is the indicator of volume changes of the sample during shear and in the case of expansion is considered positive [2–4].

The authors of [5] stated that the friction angle defined by the slope of the strength envelope consists of two components, interparticle sliding friction and geometrical interference. The geometrical interference itself is governed by dilation (or particle climbing), particle pushing, and rearrangement. Dilatancy decreases with increasing normal stress and therefore the friction angle decreases. The author of [6] explained the effect of the normal stress-friction angle relationship on the stability analysis of a rockfill dam and concluded that by considering this effect, the height of the rockfill dam could be increased. The authors of [5] expressed that the

*Correspondence: hosseini_ymail@yahoo.com

secant friction angle is a convenient parameter for expressing a curved strength envelope for granular soils and it depends on the magnitude of effective confining stress. They used existing data on the drained shear strength of granular soils to prepare a diagram that revealed the relationship between secant friction angle, effective normal stress, and initial porosity. The author of [7] presented analytical expressions for the nonlinear envelopes in terms of effective stress; classified them into three major groups as power, logarithmic, and hyperbolic types; and concluded that the failure envelope of the hyperbolic type is applicable in a wider range of stresses. The author of [8] offered a constitutive model for studying the uplift behavior of anchors in cohesionless soils in which the effect of normal stress on friction angle was taken into account. The author of [9] performed direct shear tests on rock pile material and concluded that the slope of the failure envelope decreased with increasing normal stress. The authors of [10] confirmed the nonlinear shape of the shear strength envelope at low stress levels ($<100$ kPa) and applied the true magnitude of mobilized shear strength in the slope stability analysis to avoid the overestimation of the factor of safety. The authors of [11] compared the influence of using linear and nonlinear envelopes in the heap leach pad stability, considering two actual cases of shear strength envelopes and cases of different height of the heap. They concluded that the linear envelope could overestimate the interface strength and therefore the factor of safety in the stability analysis, especially when very tall heap leach pads are analyzed (taller than 150 m), increasingly common in mining, where the vertical stress could be very high, much higher than the capacity of the large-scale direct shear equipment.

## 2. Materials

In this study, three types of sands were used, poorly graded sand from Babolsar (a town in northern Iran) because of numerous projects in that region, standard Ottawa sand in order to compare the results, and a sand with grain-size distribution similar to fine-grained filter of earth dams. Babolsar and Ottawa sands are subrounded and mainly composed of quartzite. The filter is angular and predominantly composed of gneiss. Properties and grain-size distribution of soils before and after the shear test are presented in Table 1 and Figure 1. As can be seen, the main difference between these soils is $D_{50}$, which implies that Babolsar sand is definitely finer than Ottawa sand and filter.

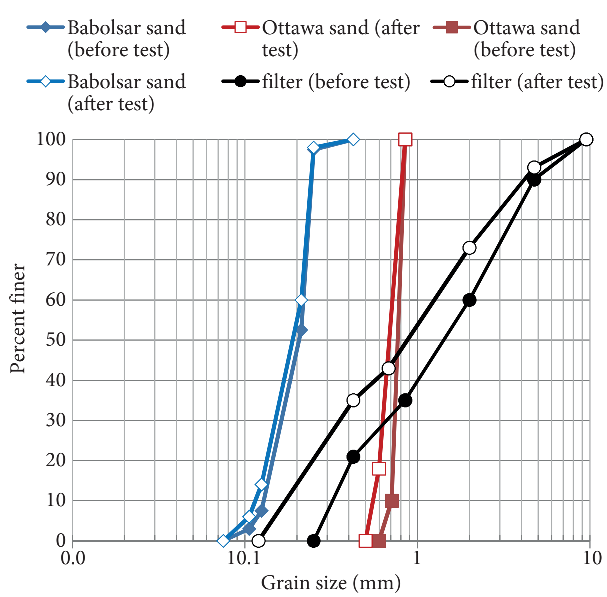


**Figure 1.** Grain-size distribution of soils before and after test.

**Table 1.** Physical properties of soils.

| Material | $C_u$ | USCS classification | $\gamma_{dmax}$ (kN/m$^3$) | $D_{50}$ (mm) | $G_s$ |
|---|---|---|---|---|---|
| Babolsar sand | 1.7 | SP | 16.68 | 0.20 | 2.772 |
| Ottawa sand [12] | 1.1 | SP | 17.00 | 0.74 | 2.660 |
| Filter | 6.3 | SP | 18.62 | 1.50 | 2.710 |

## 3. Experimental program

The samples were prepared by insertion of a specific dry mass of soil in three layers and compaction of each layer in such a way that the required dry density was achieved. Saturation of samples was done by immersing the shear box in water for 1 h. Particle-size analysis, specific gravity, standard proctor, and direct shear tests were performed according to ASTM International. The shear speeds of tests were determined based on trial and error to certify that they had no noticeable effect on the results and were selected as 0.50 $\frac{mm}{min}$ and 0.25 $\frac{mm}{min}$ for air-dried and saturated samples, respectively. The air-dried samples of Babolsar sand were tested at relative compactions ($R_d$) of 93% ($\frac{\gamma_d}{\gamma_{dmax}}$=0.93), 97%, and 100%; the air-dried samples of Ottawa sand were tested at relative compaction of 93%; the air-dried and saturated samples of filter were tested at relative compactions of 93%, 97%, and 100%; and all tests were carried out under different normal stresses of 1, 2, 4, 8, and 16 kg/cm$^2$.

## 4. Test results

In this part, results of tests and comparisons between them are presented.

### 4.1. Failure envelope

Failure envelopes of Babolsar sand, Ottawa sand, dry filter, and saturated filter at all relative compactions are shown in Figures 2a–2d, 3a–3c, and 4a–4c, and plots of shear stress against horizontal displacement for these soils at the relative compaction of 93% are shown in Figures 5a–5d. Shear tests were done in a square box of 15 × 15 cm and shear displacements were continued to 20% of box dimensions (3 cm).

As can be seen from these figures, the nonlinear regression provided a very good fit to the data and it is recommended. Failure envelopes were used to calculate the variation of $\varphi$ with $\sigma_v$. For all soils, a second-degree polynomial with zero intercept and power functions were selected as nonlinear failure envelopes because of higher correlation factors. As can be seen, the curved envelope of Babolsar sand almost matches the linear envelope, while for Ottawa sand and filter, the difference between the two types of envelopes is obvious. The reason is that with increasing normal stress, the grains of Ottawa sand and filter are significantly crushed during shear and dilatancy decreases, but for Babolsar sand this phenomenon can be ignored.

Equations resulting from linear and nonlinear regression (second-degree polynomial) for tested soils at relative compaction of 93% are summarized in Table 2.

**Table 2.** Envelope equations for linear and nonlinear regression ($R_d$ = 93%).

| Soil | Nonlinear regression | Linear regression |
|---|---|---|
| Babolsar sand | $\tau = -0.002\sigma_v^2 + 0.790\sigma_v$ ($R^2$ = 0.9999) | $\tau = 0.752\sigma_v + 0.062$ ($R^2$ = 0.9996) |
| Ottawa sand | $\tau = -0.016\sigma_v^2 + 1.095\sigma_v$ ($R^2$ = 1.000) | $\tau = 0.809\sigma_v + 0.661$ ($R^2$ = 0.994) |
| Dry filter | $\tau = -0.019\sigma_v^2 + 1.215\sigma_v$ ($R^2$ = 1.000) | $\tau = 0.881\sigma_v + 0.758$ ($R^2$ = 0.993) |
| Saturated filter | $\tau = -0.020\sigma_v^2 + 1.192\sigma_v$ ($R^2$ = 1.000) | $\tau = 0.842\sigma_v + 0.764$ ($R^2$ = 0.990) |

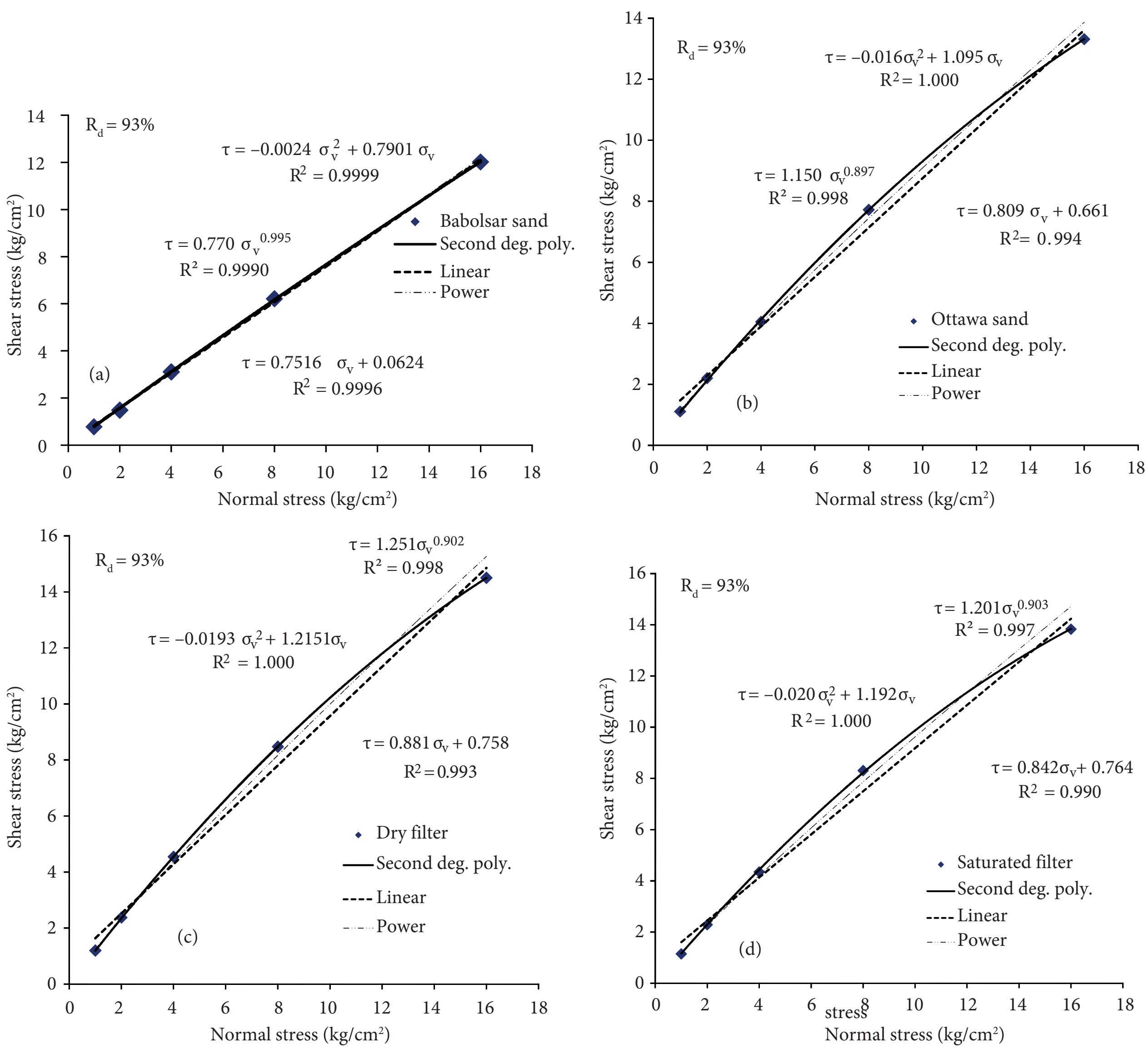


**Figure 2.** Linear and nonlinear regression of failure envelope ($R_d$ = 93%) for (a) Babolsar sand, (b) Ottawa sand, (c) dry filter, and (d) saturated filter.

In these equations, $\tau$ and $\sigma_v$ are shear and normal stresses in kg/cm$^2$, respectively. Regarding the fact that all materials are completely sandy, intercepts of linear envelopes (cohesion) are expected to be approximately zero. In linear regression, the cohesion achieved for Babolsar sand was almost negligible: 0.062 kg/cm$^2$, which can be accepted, while the cohesion achieved for Ottawa sand and filter were 0.661 kg/cm$^2$ and 0.758 kg/cm$^2$, respectively, which cannot be accepted for sands. At high normal stresses, particle crushing occurs and the linear envelope crosses the vertical axis at a higher value of cohesion.

### 4.2. Variation of secant friction angle with normal stress and relative compaction

Using nonlinear failure envelopes, values of the secant friction angle were calculated at each normal stress and relative compaction, and then by using the data fitting method twice, two variable functions of $\varphi$ were defined

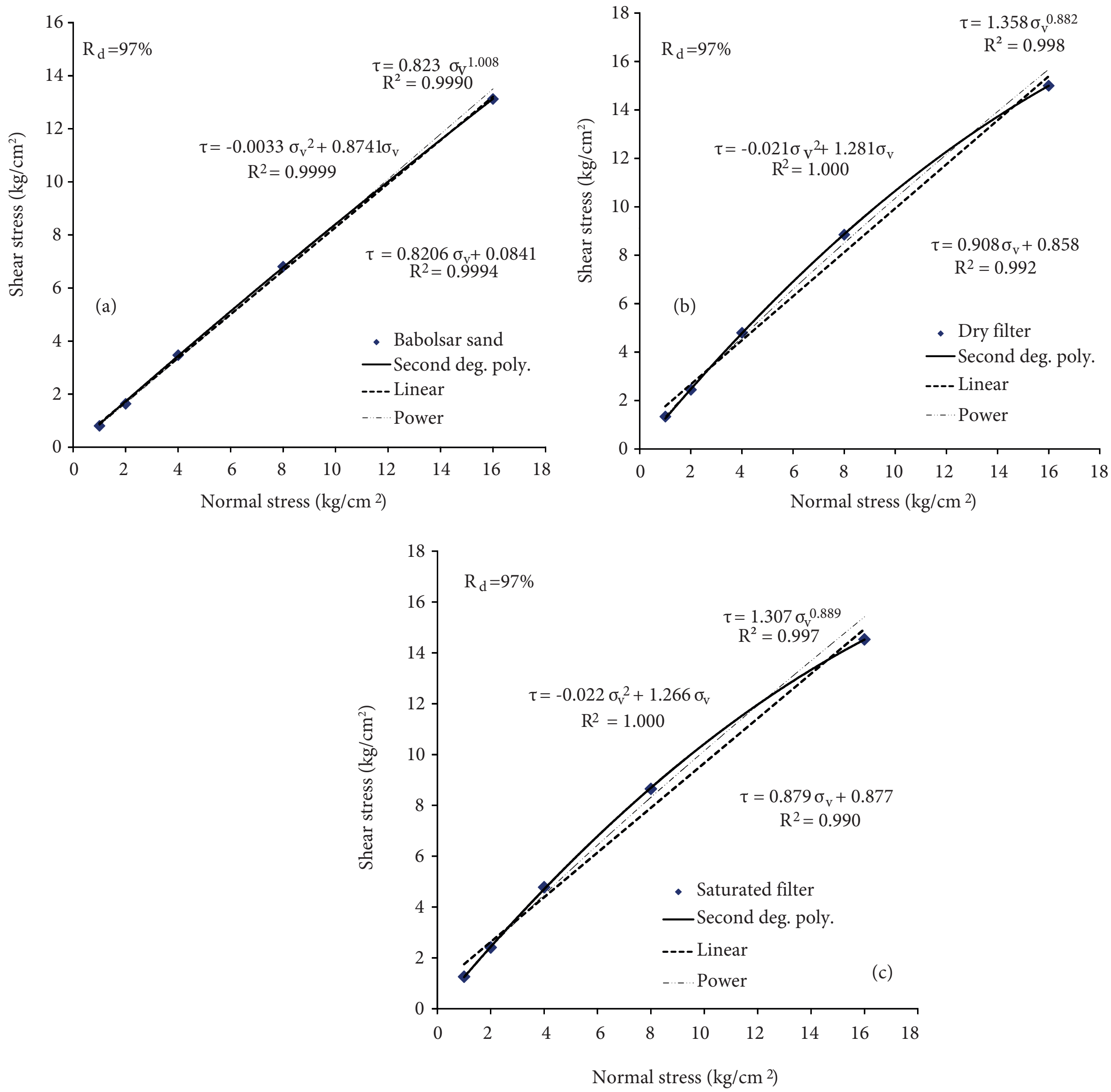


**Figure 3.** Linear and nonlinear regression of failure envelope ($R_d$= 97%) for (a) Babolsar sand, (b) dry filter, and (c) saturated filter.

in terms of $\sigma_v$ and $R_d$. In order to reach these functions, the general form of the $\varphi$ function in terms of $\sigma_v$ that better fits the data was first determined. Coefficients and constants of the achieved general function were then obtained in terms of $R_d$ by performing another data fitting since each relative compaction corresponds to specific coefficients and constants. Finally, parametric coefficients and constants in step one were replaced by $R_d$ functions expressed in step two. The results are tabulated in Table 3.

In these equations $\varphi$ is the secant friction angle in degrees, $R_d$ is the relative compaction (decimal), and $\sigma_v$ is the normal stress in kg/cm$^2$. These equations were plotted and are shown for Babolsar sand, dry filter, and saturated filter in Figures 6, 7, and 8, respectively. It can be seen from these figures that secant friction angle decreases with increasing normal stress and decreasing relative compaction. For instance, at relative compaction of 93%, secant friction angles of Babolsar sand, dry filter, and saturated filter decreased

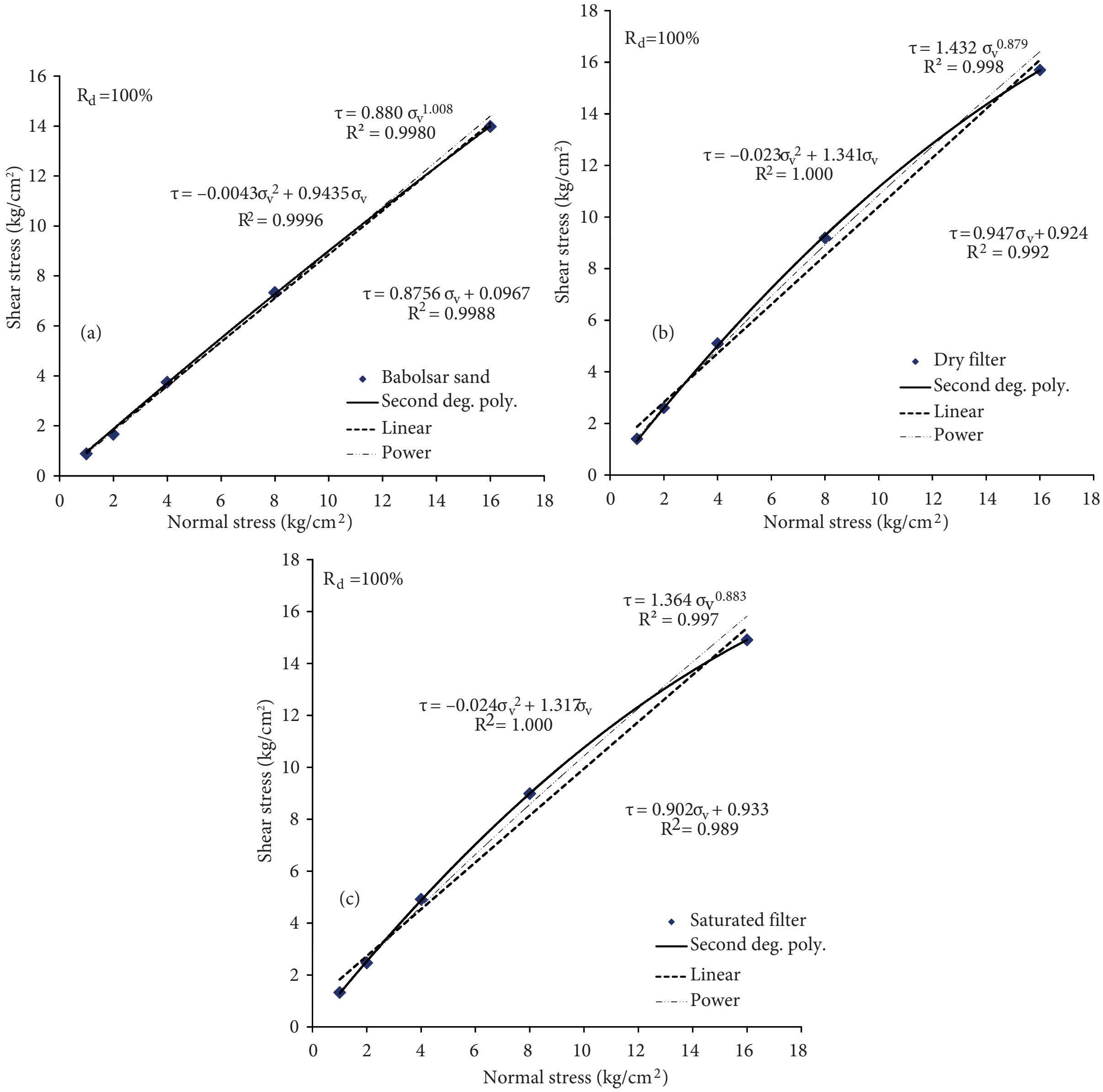


**Figure 4.** Linear and nonlinear regression of failure envelope ( $R_d$=100%) for (a) Babolsar sand, (b) dry filter, and (c) saturated filter.

**Table 3.** Two variable functions of $\varphi$ in terms of $\sigma_v$ and $R_d$.

| Soil | Function |
|---|---|
| Babolsar sand | $\phi = (-7.857R_d^2 + 13.67R_d - 6.101)\sigma_v + (72.24R_d - 28.87)$ |
| Dry filter | $\phi = (-1.309R_d^2 + 2.413R_d - 1.134)\sigma_v^2 +$<br>$(-5.119R_d^2 + 9.551R_d - 5.309)\sigma_v + (69.04R_d^2 - 94.69R_d + 78.84)$ |
| Saturated filter | $\phi = (-0.595R_d^2 + 1.006R_d - 0.445)\sigma_v^2 +$<br>$(-7.142R_d^2 + 13.37R_d - 7.161)\sigma_v + (-82.14R_d^2 + 197.8R_d - 62.97)$ |

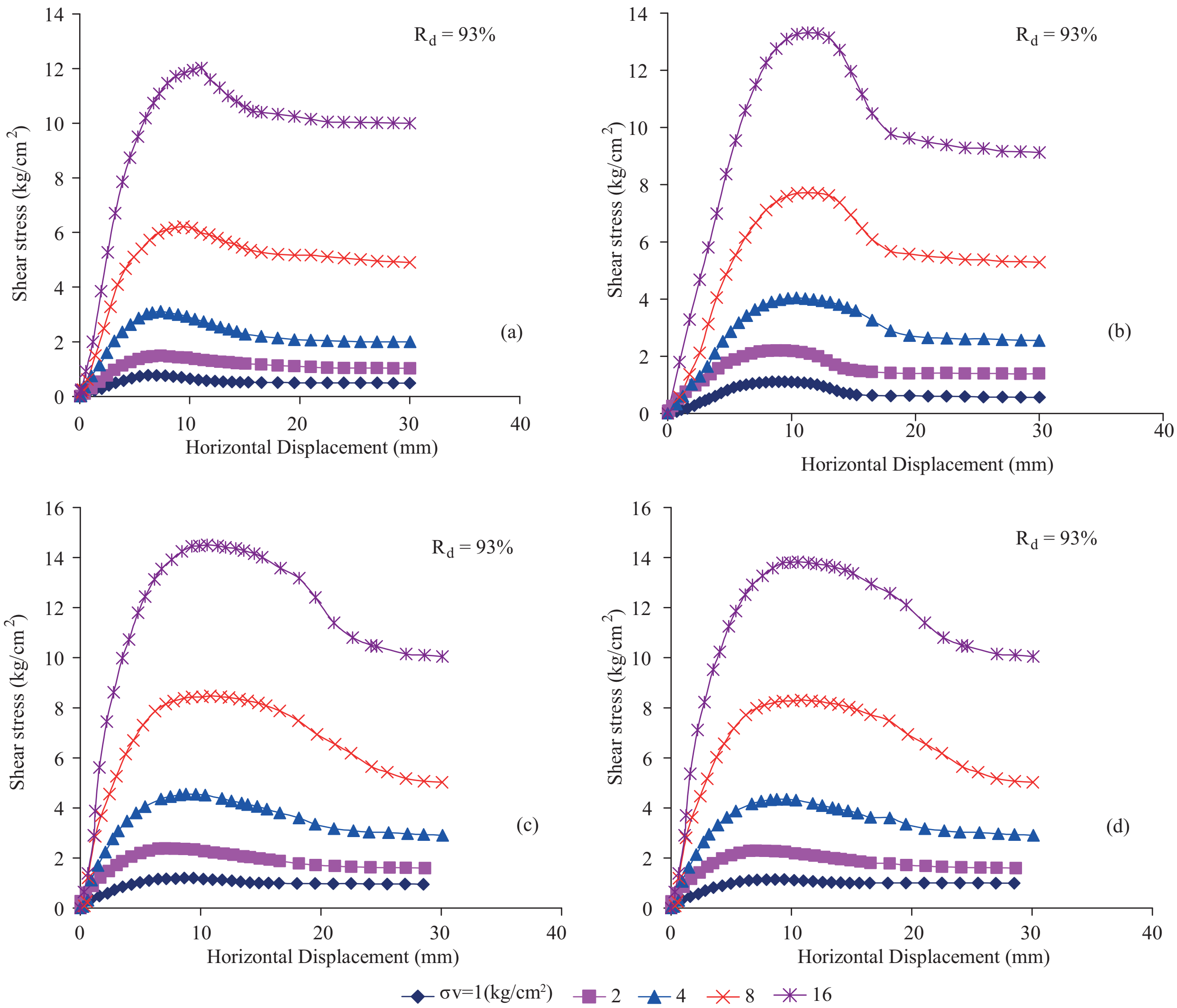


**Figure 5.** Shear stress versus horizontal displacement ( $R_d = 93\%$) for (a) Babolsar sand, (b) Ottawa sand, (c) dry filter, and (d) saturated filter.

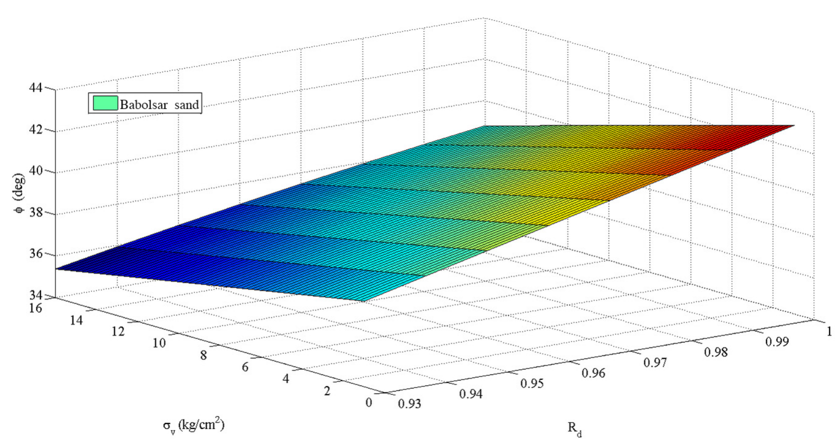


**Figure 6.** Dependence of $\varphi$ on $\sigma_v$ and $R_d$ for Babolsar sand.

3° (from 38° to 35°), 19° (from 50° to 31°), and 20° (from 49° to 29°), respectively, as the normal stress increased from 1 kg/cm$^2$ to 16 kg/cm$^2$. In other words, due to the 15 times increase in $\sigma_v$, secant friction angles of Babolsar sand, dry filter, and saturated filter decreased by about 8%, 38%, and 41%, respectively. At normal stress of 1 kg/cm$^2$, secant friction angles of Babolsar sand, dry filter, and saturated filter increased 5° (from 38° to 43°), 3° (from 50° to 53°), and 3° (from 49° to 52°), respectively, as the relative compaction increased from 93% to 100%. All secant friction angles obtained for Babolsar sand, dry filter, and saturated filter using the second-degree polynomial failure envelope are summarized in Table 4. It should be noted that the aforementioned function could not be achieved for Ottawa sand because this soil was not the main material of the current study and was only tested at a relative compaction of 93% for comparison of results.

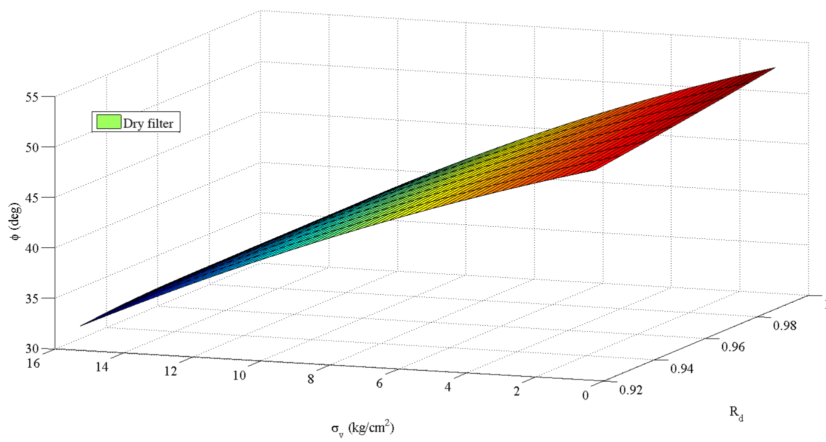


**Figure 7.** Dependence of $\varphi$ on $\sigma_v$ and $R_d$ for dry filter.

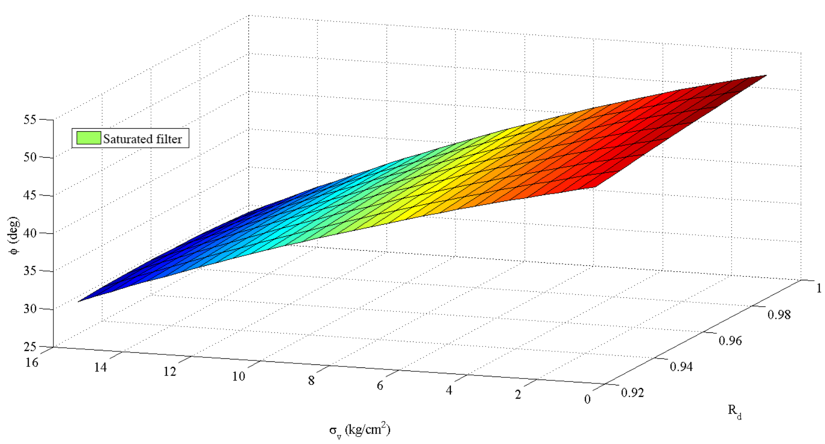


**Figure 8.** Dependence of $\varphi$ on $\sigma_v$ and $R_d$ for saturated filter.

## 5. Conclusion

In this study, the effect of normal stress and relative compaction on secant friction angles of Babolsar sand, Ottawa sand, and sand with grain-size distribution similar to the fine-grained filter of earth dams was investigated. Using test results, the following conclusions can be made:

**Table 4.** Friction angles obtained using second-degree polynomial failure envelope.

| Soil | $R_d$= 100% | $R_d$= 97% | $R_d$= 93% | Normal stress (kg/cm$^2$) |
|---|---|---|---|---|
| Babolsar sand | 40.1 | 40.9 | 38.1 | 1 |
| | 42.8 | 40.7 | 38.0 | 2 |
| | 42.3 | 40.3 | 37.6 | 4 |
| | 41.2 | 39.4 | 36.9 | 8 |
| | 38.9 | 37.5 | 35.5 | 16 |
| Ottawa sand | - | - | 46.7 | 1 |
| | - | - | 45.9 | 2 |
| | - | - | 44.0 | 4 |
| | - | - | 40.0 | 8 |
| | - | - | 30.2 | 16 |
| Dry filter | 52.3 | 51.1 | 49.6 | 1 |
| | 51.3 | 50.1 | 48.7 | 2 |
| | 49.2 | 48.1 | 46.7 | 4 |
| | 44.2 | 43.4 | 42.2 | 8 |
| | 31.2 | 31.3 | 30.9 | 16 |
| Saturated filter | 51.8 | 50.7 | 49.0 | 1 |
| | 50.7 | 49.7 | 48.0 | 2 |
| | 48.4 | 47.5 | 45.9 | 4 |
| | 43.0 | 42.4 | 41.1 | 8 |
| | 28.8 | 29.3 | 28.9 | 16 |

- Secant friction angle decreases with increasing normal stress. For instance, at relative compaction of 93%, secant friction angles of Babolsar sand, dry filter, and saturated filter decreased 3° (from 38° to 35°), 19° (from 50° to 31°), and 20° (from 49° to 29°), respectively, as the normal stress increased from 1 kg/cm$^2$ to 16 kg/cm$^2$. In other words, due to a 15 times increase in $\sigma_v$, secant friction angles of Babolsar sand, dry filter, and saturated filter decreased by about 8%, 38%, and 41%, respectively.

- Secant friction angle increases with increasing relative compaction. For instance, at normal stress of 1 kg/cm$^2$, secant friction angles of Babolsar sand, dry filter, and saturated filter increased 5° (from 38° to 43°), 3° (from 50° to 53°), and 3° (from 49° to 52°), respectively, as the relative compaction increased from 93% to 100%.

- It seems that the difference between the curved envelope and linear envelope increased with increasing $D_{50}$ (mean particle diameter), but more study is required because there are other factors influencing the results such as fine content and mineralogy.

- With increasing $D_{50}$, decrease in secant friction angle became more noticeable, because grain crushing increased and dilatancy became more limited.

- Saturating the specimens caused the nonlinear envelopes to have more curvature, and so decrease in secant friction angles increased. It also caused the linear envelopes to have smaller $\varphi$ and larger $c$ values compared with linear envelopes of air-dried specimens, as expected.

- Diagrams of secant friction angle versus normal stress were linear with good approximation.

- The two proposed variable functions can be used to estimate the secant friction angle of studied soils under the tested conditions by substituting the values of normal stress and relative compaction, and therefore no additional test is needed.
- It is better to use the curved envelope instead of the linear envelope for sands, because it provides a much better fit to the data.

## References

[1] Taylor DW. Fundamentals of Soil Mechanics. New York, NY, USA: John Wiley; 1948.

[2] Charles JA, Watts KS. The influence of confining pressure on the shear strength of compacted rockfill. Geotechnique 1980; 30: 353–367.

[3] Barton N, Kjaernsli B. Shear strength of rockfill. J Geotech Engng Div 1981; 107: 873–891.

[4] Bolton MD. The strength and dilatancy of sands. Geotechnique 1986; 36: 65–78.

[5] Terzaghi K, Peck RB, Mesri G. Soil Mechanics in Engineering Practice. 3rd ed. New York, NY, USA: John Wiley; 1996.

[6] Indraratna B. The effect of normal stress-friction angle relationship on the stability analysis of a rockfill dam. Geotechnical and Geological Engineering 1994; 12: 113–121.

[7] Maksimovic M. A family of nonlinear failure envelopes for non-cemented soils and rock discontinuities. Electronic Journal of Geotechnical Engineering 2002; 7: 3–8.

[8] Hsu ST. A constitutive model for the uplift behavior of anchors in cohesionless soils. J Chin Inst Eng 2005; 28: 305–317.

[9] Linero S, Palma C, Apablaza R. Geotechnical characterization of waste material in very high dumps with large scale triaxial testing. In: Potvin Y, editor. Proceedings of International Symposium on Rock Slope Stability in Open Pit Mining and Civil Engineering. Perth, Australia; 2007. pp. 59–75 .

[10] MD Noor MJ, Derahman A. Curvi-linear shear strength envelope for granitic residual soil grade VI. In: Jotisankasa, A, editor. Proceedings of Unsaturated Soils, Vol. 1. Pattaya, Thailand; 2011. pp. 212–217.

[11] Parra D, Valdivia R, Soto C. Analysis of shear strength non-linear envelopes of soil-geomembrane interface and its influence in the heap leach pad stability. In: Bathurst R, editor. Proceedings of Second Pan American Geosynthetics Conference & Exhibition, GeoAmericas. Lima, Peru; 2012. pp. 449–456.

[12] Das BM. Advanced Soil Mechanics. 1st ed. New York, NY, USA: McGraw-Hill; 1983.